# Adsorption of Proteins to Hydrophobic Sites on Mixed Self-Assembled Monolayers†

Emanuele Ostuni, Bartosz A. Grzybowski, Milan Mrksich, Carmichael S. Roberts, and George M. Whitesides*

*Department of Chemistry and Chemical Biology, Harvard University, 12 Oxford Street, Cambridge, Massachusetts 02138*

*Received July 18, 2002. In Final Form: November 18, 2002*

This paper describes a technique that uses mixed self-assembled monolayers of two alkanethiolates ($^{-}S(CH_2)_{11}(OCH_2CH_2)_6OR$, R = a hydrophobic group, and $^{-}S(CH_2)_{11}(OCH_2CH_2)_nOH$, $n$ = 3, 6, $EG_nOH$), in combination with surface plasmon resonance spectroscopy, to study the influence of the size and shape of R, and its density at the surface, on the hydrophobic adsorption of proteins at solid−liquid interfaces. Detailed results were obtained for $\beta$-galactosidase, carbonic anhydrase, lysozyme, and RNase A using R = $C(C_6H_5)_3$, $CH(C_6H_5)_2$, and $CH_2(C_6H_5)$. A hard-sphere model is used to rationalize the adsorption; this model, although very approximate, helps to interpret qualitative trends in the data. Using this model, the extent to which adsorbed proteins undergo conformational rearrangements appears to depend on the density of the hydrophobic groups at the surface and on the concentration of protein in solution. This paper describes the first step toward the development of a system that will allow the study of hydrophobic interactions of proteins with surfaces presenting organic groups of well-defined shape.

## Introduction

This paper introduces a model system for studying the adsorption of proteins to surfaces that present structurally well-defined hydrophobic groups at surfaces that are otherwise terminated with groups resistant to the adsorption of proteins. We used mixed self-assembled monolayers (SAMs) of alkanethiolates to generate the required surfaces (Figure 1). In this system, the proteins interacted predominantly, or exclusively, with the hydrophobic groups. Both the molecular surface area and the surface density of the hydrophobic sites influenced the extent of adsorption of each protein. At sufficiently low surface densities of the hydrophobic groups, we expected the groups to be statistically unclustered and their interactions with the protein isolated. The adsorption of proteins to surfaces that presented low mole fractions of the hydrophobic groups correlated with both the accessible hydrophobic surface of the groups and the molecular weight of the protein.

The system we describe here allows an estimate of the average number of hydrophobic groups required to cause the adsorption of a protein to the SAMs. We infer that an aggregate hydrophobic surface equivalent in area to approximately six trityl groups is required for adsorption of carbonic anhydrase. Our results also support the hypothesis that surfaces composed predominantly of hydrophobic groups promote more conformational changes in the adsorbed proteins than surfaces that present low densities of hydrophobic groups, probably because the proteins on very hydrophobic surfaces denature and spread, forming a thinner film than those on less hydrophobic surfaces that cause less extensive denaturation and structural rearrangement of the protein.

The study of protein adsorption on surfaces has historically been a difficult one. The heterogeneity of most surfaces, the heterogeneity, plasticity, and tendency to denature of proteins, the potential for microphase separation on surfaces, the potential for intermolecular interaction among proteins, and the complicating influence of buffers have all contributed to the difficulty in the field. The work described here has not yet provided a completely defined system, but it suggests that the use of SAMs that do *not* adsorb proteins, combined with the presentation of discrete hydrophobic groups at the surface of these SAMs, simplifies the experimental system substantially. Surface plasmon resonance (SPR) spectroscopy makes it possible to measure protein adsorption conveniently, although this technique is intrinsically relatively limited in the information it provides. Working at *low* surface coverage of hydrophobic groups (a regime that we have only begun to explore in this work) plausibly minimizes the influence of microphase separation and lateral interactions between hydrophobic groups. We have not begun to explore the influence of the fluid medium on adsorption. This work should, thus, be considered as a first step in reducing the complexity of a very difficult experimental problem, rather than as the final definition of a fully tractable system.

**Historical Background: Adsorption of Proteins to Surfaces and Initial Efforts to Study this Process.** Studies of the adsorption of proteins to surfaces were originally motivated by practical concerns in bioengineering, with particular emphasis on the design of biocompatible materials.[1] A wide range of materials are important in bioengineering ($Ti/TiO_2$, steel, ceramics, pyrolytic carbon, and many types of organic polymers and plasma-deposited organic thin films), but the most important class, and that with the greatest variability in surface properties, is polymers.[1] Studies of the adsorption of proteins to polymers have always been difficult, and their interpretation ambiguous, both because the composition and structure of the surfaces of most polymers is undefined at the molecular level and because it has been impossible to limit and define the region of the surface

* Corresponding author. Telephone: (617) 495-9430. Fax: (617) 495-9857. E-mail: gwhitesides@gmwgroup.harvard.edu.

† Part of the *Langmuir* special issue entitled The Biomolecular Interface.

(1) Ratner, B. D.; Hoffmann, F. J.; Schoen, J. E.; Lemon, F. *Biomaterials Science. An Introduction to Materials in Medicine*; Academic Press: New York, 1996.

10.1021/la020649c CCC: $25.00 
Published on Web 01/17/2003

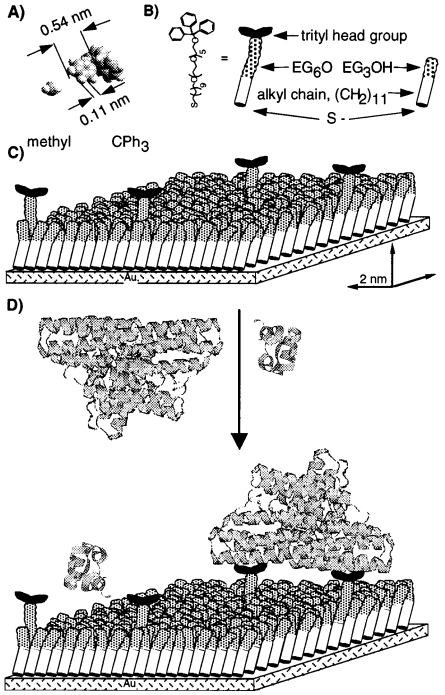


**Figure 1.** Schematic drawing illustrating the adsorption of proteins onto mixed SAMs. The components of the system are drawn approximately to scale using their van der Waals radii; the purpose of the figure is to suggest sizes of molecules and spacing between them rather than specific mechanisms of adsorption or conformations of the groups involved. (A) Space filling model (top view) of a trityl and a methyl group. (B) Model of the alkanethiol presenting a hydrophobic $CPh_3$ group. (C) Mixed SAMs prepared from this alkanethiol and an alkanethiol terminated in tri(ethylene glycol) groups present hydrophobic "patches" in a surface that otherwise does not adsorb protein. (D) At low mole fractions of $CPh_3$ (ca. $\chi_{CPh_3} = 0.01$ in this representation), only large proteins can make a sufficient number of hydrophobic contacts to adsorb. We use the ribbon structures of hemerythrin (large, MW = 108 kD) and insulin (small, MW = 5.7 kD) to represent two proteins of different sizes. We depict a single domain of gold without grain boundaries or imperfections, for simplicity, but such defects occur in gold films (with unknown influence on the adsorption of proteins). We do not know how the trityl groups are oriented relative to the plane of the interface or how they interact with the protein molecules.

with which the protein interacts.[2,3] In fact, almost every feature of these systems is undefined: the structure of the polymer surface before and after adsorption, the area of the surface that was involved, and the structure (or range of structures) of the protein after adsorption. An important qualitative conclusion from this body of work is, however, that (at least for the surfaces of most uncharged substrates) the hydrophobic effect was the dominant interaction between surface and protein.[4] Current inability to prepare and study surfaces that present structurally well-defined hydrophobic sites has limited progress in establishing structure−property relationships that describe the hydrophobic adsorption of proteins at surfaces.

**Adsorption of Proteins to Hydrophobic Surfaces.** In the most qualitative picture of adsorption, an initial event (presumably involving interaction of a hydrophobic patch on the surface of the protein and a hydrophobic region on the surface) is followed by conformational changes in the protein that expose its hydrophobic core to the hydrophobic surface (Figure 2A). Dehydration of hydrophobic surfaces (both the SAM and the protein) provides an entropic driving force for adsorption.

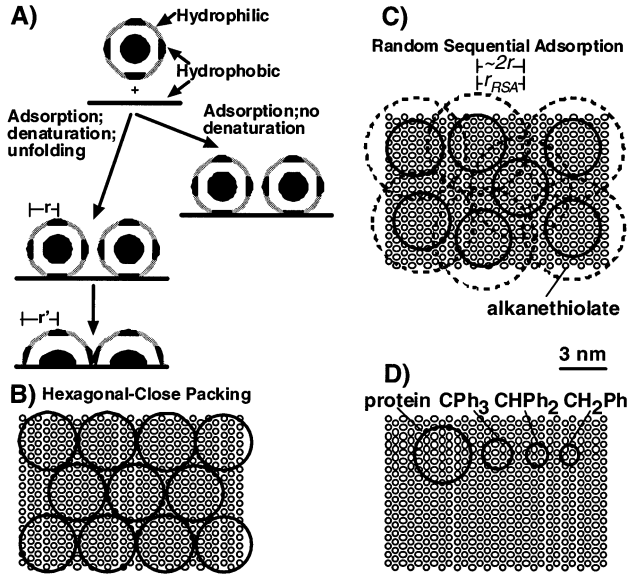


**Figure 2.** Schematic illustration of the adsorption of proteins to hydrophobic surfaces. (A) Proteins may adsorb to a surface and maintain their conformation; alternatively, proteins may adsorb in their native conformation and then spread on the surface. It is also possible for the proteins to adsorb in their native conformations and then undergo conformational changes on the surface. Hydrophobic regions of the proteins are indicated schematically in black; the proteins were drawn so as to have approximately the same volumes. We illustrate the values of $r$, $r'$, and $r_{RSA}$ that we use later in the discussion of the hard-sphere model. The adsorbed proteins are drawn as hemispheres for simplicity; we do not intend to suggest the details of the shape of the adsorbed proteins. We do assume, however, that the shape of the projection of the adsorbed proteins is circular. (B) Schematic illustration of the adsorption of lysozyme to a SAM in a HCP monolayer; we treat the protein as a hard sphere. The small empty circles represent the lattice sites of the terminal groups in a SAM. The large empty circles represent the approximate projection of the hard sphere (Table 1). (C) We illustrate the maximum coverage of the surface that can be achieved in the RSA model (54% of the surface). The dashed circles indicate the excluded area of each hard sphere. The rest of the illustration is the same as in (B). The relative areas occupied by the various circles are meant to be approximately to scale. (D) Schematic illustration of the solvent-accessible areas of the hydrophobic groups used in this study; the areas were calculated using the Quanta 4.0 software package (Molecular Simulations, MA) with a probe radius of 1.4 Å (water) and 20 dots/Å$^2$. The program calculates the area of the entire molecule, including the face of the molecule that is closer to the $(EG)_nOH$ layer and hidden (we assume) from the protein. The functional groups were treated as single molecules bound to a methoxy group representing the $(EG)_nOH$ group.

The adsorption of proteins to hydrophobic surfaces is a problem that is interesting in biophysics and relevant to biotechnology: examples of systems that require control of hydrophobic adsorption of proteins at surfaces include contact lenses, implants, systems for the purification of proteins (chromatography), and substrates for enzyme-linked immunosorbent assays (ELISA). Recent developments in microfluidic systems and high-throughput assays,[5,6] proteomics,[7] and bioanalytical devices[5,6] also require understanding of hydrophobic effects at surfaces.

(2) Elwing, H.; Welin, S.; Askendahl, A.; Lundstrom, I. *J. Colloid Interface Sci.* **1988**, *123*, 306−308.
(3) Jennissen, H. P. *J. Colloid Interface Sci.* **1986**, *111*, 570−586.
(4) Norde, W. *Driving Forces for Protein Adsorption at Solid Surfaces*; Malmsten, M., Ed.; Marcel Dekker: New York, 1998; Vol. 75, pp 27−54.

**Adsorption of Proteins to SAMs.** To circumvent the ambiguities that come with studying adsorption of proteins to heterogeneous surfaces that are undefined at the molecular level, we and others have used SAMs because they provide superb control over the properties and the structure of a surface.[8] The surfaces of metals and metal oxides are also atomically well-defined, but they generally have high interfacial free energies and do not model organic surfaces; the adsorption of proteins to these surfaces have been studied by many techniques, and they have been described extensively elsewhere.[9−17]

In an initial study, using several structurally different SAMs, we found that the amount of adsorbed protein correlated *roughly* with the values of the advancing contact angle of water on the surfaces: in that study, the nature of the correlation varied substantially with the protein. The range of surfaces with high free energies that were available for study were also limited.[18] After completing this study, however, we do not claim or believe that there is a general correlation between macroscopic properties such as wettability and protein adsorption. We have three reasons for discarding this type of correlation. (i) Although it is true that strongly hydrophobic surfaces adsorb proteins, it is not true, in general, that hydrophilic surfaces do not. In particular, charged surfaces (which are strongly hydrophilic) adsorb proteins of the opposite charge strongly. (ii) The surfaces that are *most* resistant to adsorption of proteins (e.g., those presenting oligo(ethylene glycol) and other groups) are intermediate in hydrophilicity.[19,20] (iii) Adsorption of proteins on surfaces, especially on heterogeneous surfaces, is intrinsically a result of local interactions. Adsorption is determined by interaction of a small area of the surface of the protein with a correspondingly small area of the surface. Parameters such as contact angle measure free energies averaged over much larger areas and do not measure the availability of these hydrophobic patches.

Kasemo has demonstrated that changes in ionic strength and pH affect the adsorption of hemoglobin and ferritin to hydrophobic surfaces of SAMs.[21] The charge on the proteins affects the packing because of, inter alia, repulsive interactions among adsorbed molecules. Kasemo also analyzed adsorption using a quartz crystal microbalance and inferred that proteins undergo structural rearrangements after adsorption; our observations here are in qualitative agreement with this inference. He also suggested that a second layer of native protein may adsorb weakly on the first, denatured layer. Other than in specific circumstances (e.g., cytochrome *c* on a sulfonate-terminated SAM[22]), we have not observed this phenomenon, but our experiments and those of Kasemo differ in a number of details and are not directly comparable.[23]

The central problem in these studies is that the area and structure involved in the adsorption is undefined. Although, for example, a methyl-terminated SAM presents only a single type of group, a $CH_3$ (or perhaps $CH_2CH_3$) group, it is impossible to define the area of the surface that is involved in the interaction with the protein. The system we describe here presents molecules with structurally well-defined hydrophobic surfaces at an interface consisting of $(EG)_nOH$ groups that, by itself, does *not* adsorb proteins. In principle, it should be possible to present hydrophobic molecules that are both large enough to cause protein adsorption and isolated from one another on the surface (although we have not yet experimentally realized this theoretical possibility).

**Nonadsorbing Surfaces.** A key part of our strategy is to use a nonadsorbing ("inert") surface as a noninteracting support for the hydrophobic groups. We and others have studied inert surfaces extensively, and a number of such SAMs are now available that resist adsorption of protein.[19,20,24,25] The first and still most inert SAMs are those terminating in $(EG)_nOH$ groups ($n \geq 3$); SAMs terminating in mannitol groups, developed by Mrksich and co-workers, are the only ones that seem to match fully the inertness of EG-terminated SAMs.[24] Grunze and co-workers have suggested that the inertness of EG-terminated SAMs is determined by the conformation of the ethylene glycol groups: coiled $(EG)_nOR$ ($R = H, CH_3$) groups render the surface inert, and $(EG)_nOR$ groups that are in the all-trans conformation generate adsorptive surfaces.[25,26] Experimental and theoretical work has led Grunze to hypothesize that the orientation of interfacial dipole moments, and the resulting structure of water at the interface, are important determinants of an inert surface.[26−28]

The mechanisms responsible for the ability of a surface to resist the adsorption of proteins are not yet completely understood and may vary according to the molecular structures of the groups presented at the surfaces. Examination of a group of ca. 60 mixed SAMs presenting a range of functional groups suggested that groups that made surfaces inert had four common features: they were (i) hydrophilic, (ii) hydrogen bond acceptors, (iii) *not* hydrogen bond donors, and (iv) overall electrically neutral.[19,20,29] The mannitol-presenting surface described by Mrksich[24] and surfaces terminated with oligo(ethylene glycol) are exceptions, in that they have many hydrogen bond donors.

(5) Duffy, D. C.; McDonald, J. C.; Schueller, O. J. A.; Whitesides, G. M. *Anal. Chem.* **1998**, *70*, 4974−4984.
(6) Manz, A.; Becker, H. *Microsystem Technology in Chemistry and Life Sciences*; Springer-Verlag: Berlin, 1998.
(7) Macbeath, G.; Schreiber, S. L. *Science* **2000**, *289*, 1760−1763.
(8) Bain, C. D.; Whitesides, G. M. *Science* **1988**, *240*, 62−63.
(9) Ivarsson, B. A.; Hegg, P. O.; Lundstroem, K. I.; Joensson, U. *Colloids Surf.* **1985**, *13*, 169−192.
(10) Eckert, R.; Jeney, S.; Horber, J. K. H. *Cell Biol. Int.* **1997**, *21*, 707−713.
(11) Knoll, W.; Matsuzawa, M.; Offenhausser, A.; Ruhe, J. *Isr. J. Chem.* **1996**, *36*, 357−369.
(12) Stoner, G. A.; Srinivasan, S. *J. Phys. Chem.* **1970**, *74*, 1088−1094.
(13) Scheller, F.; Jaenchen, M.; Pruemke, H. J. *Biopolymers* **1975**, *14*, 1553−1563.
(14) Murray, B. S.; Cros, L. *Colloids Surf., B* **1998**, *10*, 227−241.
(15) Jackson, D. R.; Omanovic, S.; Roscoe, S. G. *Langmuir* **2000**, *16*, 5449−5457.
(16) Cabilio, N. R.; Omanovic, S.; Roscoe, S. G. *Langmuir* **2000**, *16*, 8480−8488.
(17) Williams, D. F.; Askill, I. N.; Smith, R. *J. Biomed. Mater. Res.* **1985**, *19*, 313−320.
(18) Sigal, G. B.; Mrksich, M.; Whitesides, G. M. *J. Am. Chem. Soc.* **1998**, *120*, 3464−3473.
(19) Chapman, R. G.; Ostuni, E.; Takayama, S.; Holmlin, R. E.; Yan, L.; Whitesides, G. M. *J. Am. Chem. Soc.* **2000**, *122*, 8303−8304.
(20) Ostuni, E.; Chapman, R. G.; Holmlin, R. E.; Takayama, S.; Whitesides, G. M. *Langmuir* **2001**, *17*, 5605−5620.
(21) Hook, F.; Rodahl, M.; Kasemo, B.; Brzezinski, P. *Proc. Natl. Acad. Sci. U.S.A.* **1998**, *95*, 12271−12276.
(22) Chen, X.; Ferrigno, R.; Holmlin, R. E.; Yang, J.; Whitesides, G. M. *Langmuir*, in press.
(23) (a) Hook, F.; Rodahl, M.; Brzezinski, P.; Kasemo, B. *J. Colloid Interface Sci.* **1998**, *208*, 63−67. (b) Hook, F.; Rodahl, M.; Brzezinski, P.; Kasemo, B. *Langmuir* **1998**, *14*, 729−734.
(24) Luk, Y.-Y.; Kato, M.; Mrksich, M. *Langmuir* **2000**, *16*, 9604−9608.
(25) Harder, P.; Grunze, M.; Dahint, R.; Whitesides, G. M.; Laibinis, P. E. *J. Phys. Chem. B* **1998**, *102*, 426−436.
(26) Feldman, K.; Hahner, G.; Spencer, N. D.; Harder, P.; Grunze, M. *J. Am. Chem. Soc.* **1999**, *121*, 10134−10141.
(27) Wang, R. L. C.; Kreuzer, H. J.; Grunze, M. *Phys. Chem. Chem. Phys.* **2000**, *2*, 3613−3622.
(28) Zolk, M.; Eisert, F.; Pipper, J.; Herrwerth, S.; Eck, W.; Buck, M.; Grunze, M. *Langmuir* **2000**, *16*, 5849−5852.
(29) Holmlin, R. E.; Chen, X.; Chapman, R. G.; Takayama, S. T.; Whitesides, G. M. *Langmuir* **2001**, *17*, 2841−2850.

$(EG)_nOH$-terminated surfaces were best suited for our needs in this work for several reasons: (i) they allow no significant adsorption (<0.2% of a monolayer) of the proteins we have examined here; (ii) the synthesis of alkanethiols that contained the hydrophobic groups connected to the $(EG)_nOH$ moiety by an ether linkage is simple; (iii) there is adequate background information on the formation of mixed SAMs with alkanethiols that contain $(EG)_nOH$ moieties.[25,26,30,31]

**Objective and Experimental Design of this Work.** The objective of this work was to develop a system based on SAMs that presented hydrophobic molecules as isolated entities at surfaces that were otherwise inert and allowed the process of adsorption to be studied conveniently (here, by SPR). Mixed SAMs that present $(EG)_3OH$ and $(EG)_6OR$ groups (Figure 1) have been used successfully in several studies of biospecific adsorption and cell adhesion.[32−35] We have studied a series of three rigid hydrophobic groups, $R = CH_2Ph$, $CHPh_2$, and $CPh_3$, presented on $(EG)_6$ spacers at the surface of a SAM otherwise comprising $(EG)_3OH$ groups (Figure 1).

The use of mixed SAMs on gold-coated substrates is compatible with detection of adsorption using SPR in the presence of buffer. The SPR spectrometer that we used is sufficiently sensitive to detect reliably the adsorption of as little as 0.2% of a monolayer of protein;[36] greater sensitivity is possible with other instrumental configurations.[37,38] SPR also makes it possible to measure adsorption at a rate that is sufficient for kinetic analysis of association and dissociation. SPR is particularly well suited for studying the hydrophobic adsorption of proteins because it does not require functionalization of the protein; SPR has been described extensively elsewhere.[34−39]

Mixed SAMs were prepared using solutions of $HS(CH_2)_{11}O(EG)_3OH$ and $HS(CH_2)_{11}O(EG)_6OR$. We *assume* that the mole fraction of the alkanethiolates in the SAM that terminate in R ($\chi_R$) is equal to the mole fraction of those groups *in solution* (eq 1).

$$\chi_R = \frac{[HS(CH_2)_{11}(EG)_nOR]}{[HS(CH_2)_{11}(EG)_nOR] + [HS(CH_2)_{11}(EG)_nOH]} \quad (1)$$

Although this assumption is certainly not exactly correct, previous work[31] suggests that deviations will be small for small values of $\chi_R$. In this paper, we are, in any event, primarily interested in *trends* with $\chi_R$, rather than in absolute values of $\chi_R$; hence, the error inherent in this assumption is not important in this work. Phase separation among the different components of the mixed SAMs may occur and will be more probable at higher values of $\chi_R$. At low surface densities of the hydrophobic group R, these individual groups would exist largely as isolated and structurally defined hydrophobic sites to which proteins in solution could adsorb.

The most interesting and mechanistically informative steady-state adsorption data will be obtained, we believe, when $\chi_R \rightarrow 0$; in this regime, phase separation of R-terminated groups is least likely to occur and it may ultimately be possible to observe the interaction of proteins with single hydrophobic groups.[30,31] In this paper, we have surveyed adsorption over the complete range of surface densities: from $\chi_R \rightarrow 0$ (where the SAMs will be ordered and the R groups isolated) to $\chi_R \rightarrow 1$ (where the surface will consist largely or entirely of the group R, probably in disordered form). By studying the adsorption as a function of $\chi_R$ between these limits, we intended to survey the characteristics of this experimental system. We also wished to be able to detect adsorption events in which more than one R group was involved.

**Analysis of the Results with the Hard-Sphere Model.** We wished to have *some* simple model against which to compare the experimental data. Rather than trying to build into the model the complexity that undoubtedly accompanies the real process of protein adsorption and conformational change,[40a] we have chosen the simplest physically relevant picture: that of hard spheres adsorbing to a planar surface.[40−42] The ways in which hard spheres pack on surfaces are well understood, and ensembles of hard spheres provide a starting point for interpreting the packing of proteins at hydrophobic SAMs.[40,41,43,44]

Protein adsorption can occur in at least two limiting ways (Figure 2A). In the first, the proteins can adsorb and then move laterally into a hexagonal close-packed (HCP) configuration; in the second, the proteins adsorb randomly and irreversibly at a site on the surface. We refer to this second model as random sequential adsorption (RSA). Figure 2B illustrates the average area of the projection of the hard sphere in a HCP monolayer; the dotted circles in Figure 2C were drawn to illustrate the excluded area, that is, the area that cannot be occupied by the center of a second sphere because it would bring the two spheres in closer contact than the hard spheres in the RSA model.

Once adsorbed, proteins can either retain their spherical shape (with radius $r$) or spread to cover a projected circular surface with radius $r'$ (Figure 2A). By comparing our results to the predictions of the hard-sphere model, we obtain a *semiquantitative* description of the adsorption of proteins to hydrophobic surfaces. This analysis suggests that proteins undergo structural rearrangements and spread upon adsorption.

## Results and Discussion

**Preparation and Characterization of Mixed SAMs.** Mixed SAMs were formed by soaking gold-coated glass substrates for 8 h in 2 mM (total thiol concentration) solutions in ethanol with the value of $\chi_R$ desired for the surface. Although we have not carried out the experiments

(30) Prime, K. L.; Whitesides, G. M. *Science* **1991**, *252*, 1164−1167.
(31) Prime, K. L.; Whitesides, G. M. *J. Am. Chem. Soc.* **1993**, *115*, 10714−10721.
(32) Mrksich, M.; Grunwell, J. R.; Whitesides, G. M. *J. Am. Chem. Soc.* **1995**, *117*, 12009−12010.
(33) Roberts, C.; Chen, C. S.; Mrksich, M.; Martichonok, V.; Ingber, D. E.; Whitesides, G. M. *J. Am. Chem. Soc.* **1998**, *120*, 6548−6555.
(34) Sigal, G. B.; Bamdad, C.; Barberis, A.; Strominger, J.; Whitesides, G. M. *Anal. Chem.* **1996**, *68*, 490−497.
(35) Lahiri, J.; Isaacs, L.; Grzybowski, B.; Carbeck, J. D.; Whitesides, G. M. *Langmuir* **1999**, *15*, 7186−7198.
(36) The instrumental limit of detection of our BIAcore 1000 instrument is approximately 10 RU; we consider a monolayer of fibrinogen with ca. 5000 RU approximately complete.
(37) Raether, H. *Surface Plasma Oscillations and Their Applications*; Hass, G., Francombe, M., Hoffman, R., Eds.; Academic Press: New York, 1977; Vol. 9, pp 145−261.
(38) Thiel, A. J.; Frutos, A. G.; Jordan, C. E.; Corn, R. M.; Smith, L. M. *Anal. Chem.* **1997**, *69*, 4948−4956.
(39) Fluorescence-based techniques require the attachment of dye molecules to the proteins to enable detection; the conjugated molecular systems of dyes add significant hydrophobic character to the surface of proteins and would probably cause dye-conjugated proteins to exhibit a different adsorption isotherm with a hydrophobic surface than unfunctionalized proteins.

(40) (a) Morra, M. *J. Biomat. Sci., Polym. Ed.* **2000**, *11*, 547−569. (b) Feder, J. *J. Theor. Biol.* **1980**, *87*, 237−254.
(41) Schaaf, P.; Talbot, J. *J. Chem. Phys.* **1989**, *91*.
(42) Schaaf, P.; Voegel, J. C.; Senger, B. *Ann. Phys.* **1998**, *23*, 1−5.
(43) Feder, J.; Giaever, I. *J. Colloid Interface Sci.* **1980**, *78*, 144−151.
(44) Hinrichsen, E. L.; Feder, J.; Jossang, T. *J. Stat. Phys.* **1986**, *44*, 793−799.

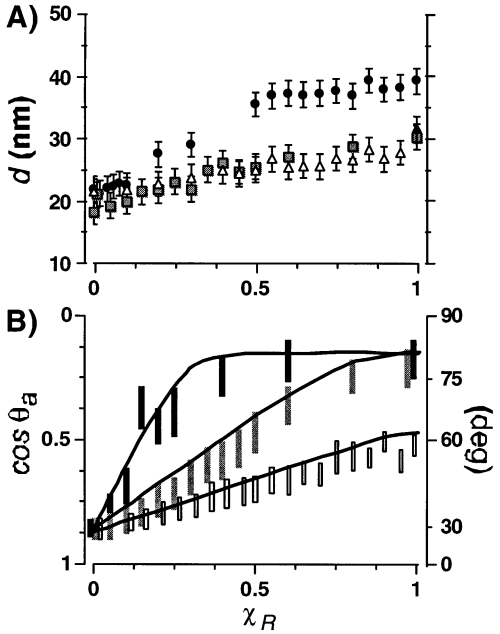


**Figure 3.** (A) Plots of the thickness $d$ (nm) (measured by ellipsometry) of mixed SAMs of $HS(CH_2)_{11}(EG)_6OR$ and $HS(CH_2)_{11}(EG)_3OH$ as a function of $\chi_R$ for R = $CPh_3$ (●), $CHPh_2$ (■), and $CH_2Ph$ (△). Each value of $d$ represents the average of ellipsometric measurements taken at three different locations on the surface of a SAM. (B) The wettability, cos $\theta$, of mixed SAMs of $HSC_{11}H_{22}(EG)_6OR$ and $HSC_{11}H_{22}(EG)_3OH$ as a function of $\chi_R$ for R = $CPh_3$ (black bars), $CHPh_2$ (gray bars), and $CH_2Ph$ (unfilled bars). The wettability is measured by the cosine of the advancing ($\theta_a$) and receding ($\theta_r$) contact angles of distilled water on these SAMs. The length of the symbol represents the hysteresis in the contact angles of water, $\cos\theta_r - \cos\theta_a$; we plot the minimum values measured for $\cos\theta_r$ and the maximum values measured for $\cos\theta_a$. Some symbols have been offset horizontally for clarity. The lines connecting the data are meant only to guide the eye. They are positioned to represent $\cos\theta_a$. We assume that they are linear for small values of $\chi_R$.

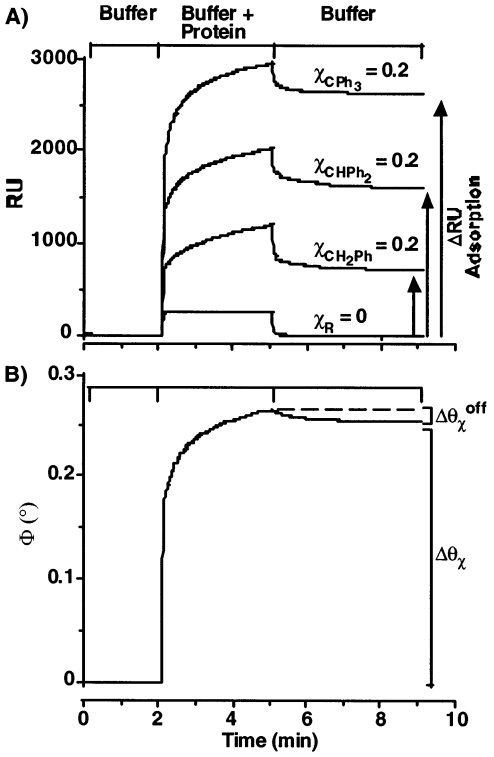


**Figure 4.** (A) SPR sensorgrams summarize the protocol normally used to measure the adsorption of proteins to surfaces and give representative data for the adsorption of $\beta$-galactosidase to mixed SAMs with $\chi_{CPh_3} = \chi_{CHPh_2} = \chi_{CH_2Ph} = 0.2$ and $\chi_R = 0$. The experimental conditions used to obtain the data are described fully in the text and in the materials and methods section. The arrows indicate the values of ΔRU that were measured on each surface. The values of ΔRU increase with increasing size of the R groups. (B) SPR sensorgram showing the adsorption of $\beta$-galactosidase to a SAM with $\chi_{CPh_3} = 0.2$ such as the one in (A). The sensorgram in this figure was obtained by subtracting from the original sensorgram, arithmetically, a sensorgram obtained by following the same protocol with the same solution of $\beta$-galactosidase on a SAM terminated only with $(EG)_3OH$ groups ($\chi_R = 0$, as in (A)). This subtraction removes the contributions to the signal from the changes in the bulk index of refraction of the solution that would interfere with the determination of the changes in the index of refraction at the surface and, therefore, with measurements of adsorption and desorption of protein. The result of the subtraction is most evident during the dissociation of the protein from the surface (compare with (A)). In this plot, we also label the quantities $\Delta\Phi_\chi^{off}$ and $\Delta\Phi_\chi$ that are used in the discussion of the dissociation of proteins from the SAMs.

that would be necessary to detect phase separation directly, we believe that, at least for values of $\chi_R < 0.1$, the extent of phase separation and the degree of disorder in our mixed SAMs are small.[8,31]

The values of the cosine of the advancing contact angle of water (a measure of wettability) and of the ellipsometric thickness of the mixed SAMs increased approximately linearly as a function of $\chi_R$ until maximum values were reached (Figure 3); we refer to the regime where maximum values are measured as "saturated". The values of the thickness and wettability reached saturation at $\chi_R < 1$ because each bulky hydrophobic group covers more projected area than the OH group of an $(EG)_3OH$ moiety in the mixed SAMs.[45]

The most informative trends in the values of the thickness and the wettability are, in principle, obtained at low values of $\chi_R$, where the SAMs are most ordered (Figure 3). Although we do not understand why the values of the thickness of mixed SAMs obtained with derivatives of $CHPh_2$ and $CH_2Ph$ groups were similar for the same values of $\chi_R$, we note that the values of $\cos\theta_a$ were markedly different for these two surfaces and agreed with our expectation that, for the same value of $\chi_R$, a mixed SAM terminated with $CHPh_2$ groups should be more hydrophobic than one terminated with $CH_2Ph$ groups (Figure 3). The increases in contact angle with values of $\chi_R$ are consistent with increases in surface free energy.

**Adsorption of Proteins.** *Experimental Protocol.* The surfaces were washed with sodium dodecyl sulfate (SDS, 10 mg/mL) for 2 min and then with phosphate-buffered saline (PBS, pH 7, 154 mM ionic strength) for 1 min and a solution of protein for 3 min; the adsorbed layer of protein was washed with buffer for 4 min (Figure 4). We did not investigate the influence of pH, buffer, ionic strength, and the duration of the flow of the solution of protein over the surface on hydrophobic adsorption in this initial study with mixed SAMs; variation of those parameters can, however, have a significant effect on the adsorption of proteins.[4,21,46] Our results and previous work from our group on the adsorption of carbonic anhydrase to mixed SAMs indicate that the adsorption processes that we investigated are not limited by mass-transport effects.[35] Previous work indicates that the amount of adsorbed

(45) The values of $\chi_R$ for which saturation is observed are approximately consistent with those calculated using the excluded volume of each R group.

(46) Cohen Stuart, M. A. *Macromolecular Adsorption*: *A Brief Introduction*; Malmsten, M., Ed.; Marcel Dekker: New York, 1998; Vol. 75, pp 1−26.

material measured by SPR increases with increasing concentration of protein in solution[47a] and that the amount of adsorbed protein measured by SPR correlates with the amounts measured with radiolabeled proteins.[47b] We studied the adsorption of $\beta$-galactosidase, carbonic anhydrase, lysozyme, and RNase A; the range of structures, sizes, and values of pI of this representative group of proteins was sufficient for a meaningful study of hydrophobic adsorption.

*Adsorption Isotherms.* The commercial Biacore instrument that we used measures the change in the angle of minimum reflection ($\Delta\phi$) of light that impinges on the substrates. The instrument uses an algorithm to track the changes in the minimum angle of reflection as a function of time; these changes are proportional to the amount of protein that adsorbs to the surface and are measured in reflection units.[37,47] Figure 4 illustrates that for a given value of $\chi_R$, the amount of adsorbed protein increased with increasing size of the R group. The difference between the value of the signal (reflection units ($\Delta$RU)) measured after and before allowing a solution of protein to flow over a SAM ($\Delta$RU, Figure 4) can be converted to a value of the change in the angle of reflection using the relationship $\Delta\phi \approx \Delta RU/10000$.

The system of mixed SAMs that we use makes it straightforward to investigate the effect of the length of the $(EG)_nOH$ ($n = 3, 6$) layer in mixed SAMs of $(EG)_nOH$ and $(EG)_6OR$ on the adsorption of protein. Past work involving biospecific adsorption at mixed SAMs has indicated that the ligand of interest had to protrude from the inert layer to interact with its binding partner with values of $K_D$ similar to those for soluble species.[32,34,48] We found no evidence that the hydrophobic adsorption of proteins was affected by the length of the inert $(EG)_nOH$ layer in the range $n = 3-6$ (Figure 5). We attribute this difference between biospecific adsorption and hydrophobic adsorption to the fact that the former requires interaction of the ligand with a deep pocket in the enzyme, while the latter requires only interaction with a hydrophobic patch on the surface of the protein. Figure 5 also shows that the shapes of the isotherms were reproducible with different batches of alkanethiols, and on different days.

It is easier to compare the adsorption of different proteins if the values of $\Delta\Phi$ are normalized. We have chosen to normalize all values of $\Delta\Phi$ for each R group to the values measured at $\chi_R = 1$, that is, the surface that presents the largest number of hydrophobic groups (Figure 3). The observation that $\Delta\Phi_\chi/\Delta\Phi_{\chi=1}$ is *greater* than 1.0 at some intermediate values of $\chi_R$ probably reflects rapid denaturation and spreading of the protein on hydrophobic surfaces (Figure 6). We discuss this observation in detail later on in the paper. Values of $\Delta\Phi_\chi/\Delta\Phi_{\chi=1}$ reached maxima at values of $\chi_R$ lower than those required to give maximum values of the thickness or of the cos $\theta_a$ of the mixed SAMs (Figure 3). We interpret these differences as suggesting that the adsorption of proteins is more sensitive to the molecular details of the surface than are ellipsometry and contact angle goniometry. It would be difficult to attempt to relate the surface free energy measured by the contact angles to the adsorption of protein for two reasons: (i) surface free energies are typically obtained from contact angles that are averaged over very large areas relative to the area of molecular contact, and (ii) the mixed SAMs used in this study are heterogeneous. In this study, and in others we have carried out, we have found that surface free energy cannot be used to predict accurately if a surface will adsorb or repel proteins; for example, a SAM terminated with hexa(ethylene glycol) has $\theta_a \sim 40°$ and it resists the adsorption of protein, while SAMs terminated with OH and $CH_3$ groups adsorb large amounts of protein (ca. 2-fold difference) and have $\theta_a \sim 10°$ and 110°, respectively.[18-20,31]

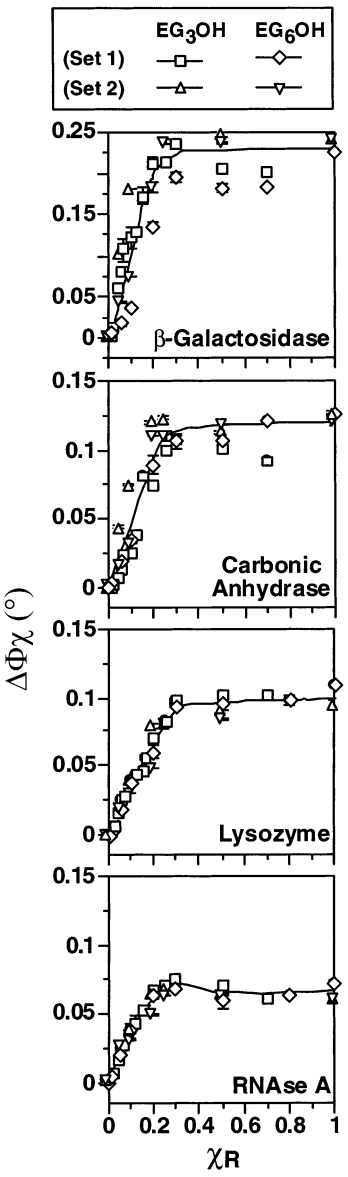


**Figure 5.** Plots of the amounts ($\Delta\Phi_\chi$) of four proteins that adsorbed to mixed SAMs as a function of the mole fraction ($\chi_R$) of the hydrophobic component $HS(CH_2)_{11}(EG)_6OCPh_3$ with two different lengths of the ethylene glycol layer: tri(ethylene glycol) (□, △; sets 1 and 2) and hexa(ethylene glycol) (◇, ▽; sets 1 and 2). The experimental conditions used to obtain the data are described in the text and in the materials and methods section. The two sets of data (set 1, set 2) were obtained using two samples of $HS(CH_2)_{11}(EG)_6OCPh_3$ that were synthesized separately, but using the same batches of $HS(CH_2)_{11}(EG)_nOH$. Each point reports the average of two measurements performed on two different areas of the same surface. The error bars represent the measured extremes; in most cases, the range is smaller than the height of each point. We have not defined the uncertainty in the values of $\chi_R$ statistically. The lines connecting the data are meant only to guide the eye.

The adsorption isotherms of $\beta$-galactosidase and carbonic anhydrase (CA) were similar on mixed SAMs terminated with $CPh_3$, $CHPh_2$, and $CH_2Ph$ groups (Figure

(47) (a) *Handbook of Biochemistry and Molecular Biology*, 3rd ed.; CRC Press: Cleveland, 1976; Vol II. (b) Stenberg, E.; Persson, B.; Roos, H.; Urbaniczky, C. *J. Colloid Interface Sci.* **1991**, *143*, 513.

(48) Houseman, B. T.; Mrksich, M. *Mol. Biol. Cell* **1998**, *9*, 2494.

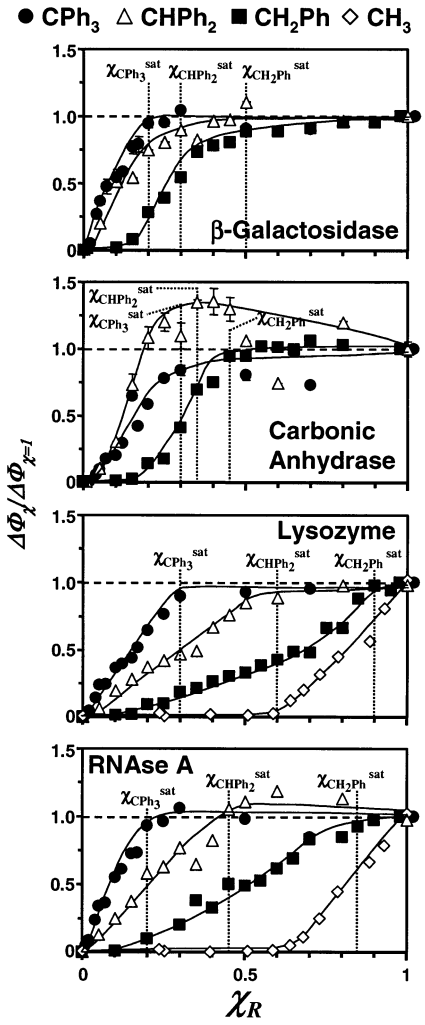


**Figure 6.** Plots of $\Delta\Phi_\chi/\Delta\Phi_{\chi=1}$ (a measure of the amount of protein adsorbed normalized to the amount adsorbed at $\chi_R = 1$) obtained using the protocol summarized in Figure 4 (see text for details) for the adsorption of $\beta$-galactosidase, carbonic anhydrase, lysozyme, and RNAse A on mixed SAMs of $HS(CH_2)_{11}(EG)_6OR$ and $HS(CH_2)_{11}(EG)_3OH$, as a function of $\chi_R$, where R = $CPh_3$ (●), $CHPh_2$ (△), and $CH_2Ph$ (■). We also plot the values of $\Delta\Phi_\chi/\Delta\Phi_{\chi=1}$ obtained by Mrksich et al. with mixed SAMs of $HS(CH_2)_{11}(EG)_3OH$ and $HS(CH_2)_{10}CH_3$ (◇) (ref 50). The error bars represent the highest and lowest values measured; in most cases, the range is smaller than the height of each point. The uncertainty in the values of $\chi_R$ is undefined. The points obtained with $\chi_R = 1$ have been offset for clarity. The lines connecting the data are drawn only to guide the eye. We label the values of $\chi_R^{sat}$ that are used in Figure 7. The values for carbonic anhydrase for $CHPh_2$ seem anomalous but were reproducible in another set of independent measurements.

6).[49] The large molecules of $\beta$-galactosidase and carbonic anhydrase probably contacted more R groups and adsorbed to a greater extent than lysozyme and RNAse at any value of $\chi_R$. For a given value of $\chi_R$, adsorption decreased as expected on the basis of exposed hydrophobic area in the order $CPh_3 > CHPh_2 > CH_2Ph$ (Figure 6). The fractional coverage of protein that was measured with mixed SAMs that presented large hydrophobic groups was always larger (except at $\chi_R = 1$), at similar values of $\chi_R$, than that measured by Mrksich et al. with mixed SAMs of $HS(CH_2)_{10}CH_3$ and $HS(CH_2)_{11}(EG)_3OH$, also expected.[50,51]

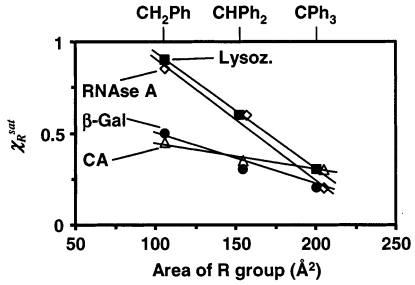


**Figure 7.** Plot of the values of $\chi_R^{sat}$ (the value of $\chi_R$ at which adsorption of protein reached saturation in Figure 6) vs the solvent-accessible area of the R groups. The values of $\chi_R^{sat}$ were chosen, by eye, as the values of $\chi_R$ at which $\Delta\Phi_\chi/\Delta\Phi_{\chi=1}$ was greater than 0.9 or reached a plateau in the plots of $\Delta\Phi_\chi/\Delta\Phi_{\chi=1}$ vs $\chi_R$ in Figure 6. Values obtained with $\beta$-galactosidase, carbonic anhydrase, lysozyme, and RNAse A are labeled as $\beta$-Gal, CA, Lysoz., and RNAse A, respectively. The solvent-accessible surface areas were calculated using the same method described in the caption of Figure 2. Some points have been offset horizontally for clarity. The lines connecting the data are drawn only to guide the eye and to suggest the relative values of the slopes; given the qualitative nature of our determination of values of $\chi_R^{sat}$, we believe that the slopes of the plots obtained for $\beta$-galactosidase and carbonic anhydrase are not statistically different from one another but are sufficiently different from those of lysozyme and RNAse.

Figures 5 and 6 indicate that the amounts of protein that adsorbed to mixed SAMs of $(EG)_3OH$ and $(EG)_6OR$ reached near-maximum values (saturation) for $\chi_R$ greater than a characteristic value for each R group ($\chi_R^{sat}$); we define $\chi_R^{sat}$ as the value of $\chi_R$ at which $\Delta\Phi_\chi$ reaches $0.9\Delta\Phi_{\chi=1}$, or where it reaches a maximum (Figure 6). This value is not sharply defined, and its choice has a subjective component. As expected, the values of $\chi_R^{sat}$ decreased with increasing size of the hydrophobic groups and with increasing molecular weight of the proteins (Figure 7). Lysozyme and RNAse, presumably because of their small size, require a higher density of hydrophobic groups to reach given values of $\Delta\Phi_\chi/\Delta\Phi_{\chi=1}$ than do $\beta$-galactosidase and carbonic anhydrase (Figure 7).

*Removal of Adsorbed Protein.* The layer of adsorbed protein could be removed from the mixed SAMs by allowing a solution of SDS (10 mg/mL) to flow over the surface for 10 min. This procedure cleaned the SAMs from the adsorbed layer of protein and made it possible to use the SAMs multiple times with reproducible results (Figure 8). The removal of adsorbed protein with SDS is consistent with hydrophobic interactions as the dominant mechanism of adsorption of proteins to these SAMs.

*Desorption of Adsorbed Proteins.* The desorption of proteins from the mixed SAMs was generally slow, and it could not be fit by a simple exponential. For example, in Figure 8, the SPR signal decreased by only 15% while washing the surface with buffer for 5 h ($k_{off} \sim 5 \times 10^{-5}$ $s^{-1}$). We believe that the extent of desorption from the layer of adsorbed protein as a function of the density of

(49) We do not understand the reasons for the shape of the plot of $\Delta\Phi\chi/\Delta\Phi\chi_{=1}$ vs $\chi_R$ obtained with carbonic anhydrase on $CHPh_2$, but we note that the overall trend was reproducible during an independent set of experiments performed with two different batches of both alkanethiols. It is possible that the diphenyl and benzyl derivatives interact with the hydrophobic regions of the binding pocket of CA; ligands with similar structures have been found to bind effectively to CA molecules. See: Gao, J., et al. *J. Med. Chem.* **1996**, *39*, 9, 1949−1955 and Avila, L. Z., et al. *J. Med. Chem.* **1993**, *36*, 126−133. This hypothesis could potentially be verified by performing the adsorption experiments in the presence of a soluble ligand that interacts specifically with the binding pocket of CA. We have, however, not carried out these experiments.

(50) The data of Mrksich et al. cannot be compared directly with those we report here because they were obtained with SAMs in which the hydrophobic groups were buried below the interface defined by the protruding inert groups, but they are useful in inferring the effects of the size and density of the ligand.

(51) Mrksich, M.; Sigal, G. B.; Whitesides, G. M. *Langmuir* **1995**, *11*, 4383−4385.

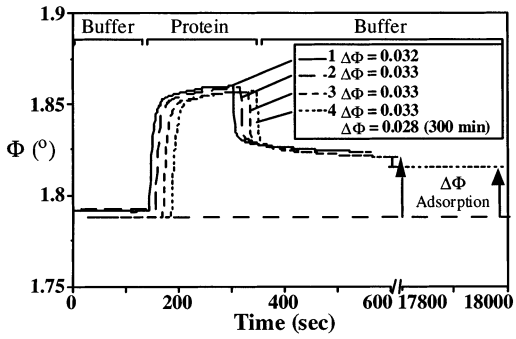


**Figure 8.** Consecutive SPR response curves for the adsorption of carbonic anhydrase (1 mg/mL) to a SAM with $\chi_{CPh_3} = 0.10$. The curves presented in this figure were obtained after depositing an initial layer of CA on the SAM and removing it by washing with SDS solution (see experimental section for details). The same procedure was repeated four times in succession (curves 1−4); a buffered (phosphate-buffered saline, pH 7.4) solution of SDS (10 mg/mL) was allowed to flow over the SAM for 15 min, followed by 2 min of buffer, to remove the previously adsorbed layer before each new injection of protein. The curves were artificially offset by 15 s for clarity. The initial SPR response of each curve reflects our ability to remove the adsorbed layer of protein with detergent and establish the same baseline after every deposition cycle. The values of ΔΦ were obtained after washing the protein layer with buffer for 240 s, unless noted otherwise. Curve 4 shows that the film of CA formed by nonspecific adsorption to a SAM of $HS(CH_2)_{11}(EG)_6$-$OCPh_3$ is fairly stable. The response decreased by only 15% over $1.75 \times 10^4$ additional seconds of washing with buffer.

hydrophobic groups can suggest the heterogeneity in the adsorbed proteins. We report the relative amounts of proteins that desorbed in terms of the percentage of the adsorbed protein that dissociated ($\Delta\Phi_\chi^{off}/\Delta\Phi_\chi \times 100$).[52] The value of ΔΦ obtained by measuring the signal decrease between the end of the flow of protein solution and the end of the buffer rinse ($\Delta\Phi_\chi^{off}$, Figure 4) was divided by the amount of protein that adsorbed to that surface ($\Delta\Phi_\chi$, Figure 4).

At values of $\chi_R < \chi_R^{sat}$, the protein molecules desorbed from the surfaces rather easily (Figure 9). The decrease in $\Delta\Phi_\chi^{off}/\Delta\Phi_\chi \times 100$ (Figure 9) as a function of $\chi_R$ is consistent with the hypothesis that as the surfaces become crowded with hydrophobic groups, the protein molecules adsorb more strongly (desorb to a smaller extent) and engage more R groups than on a surface that presents well-spaced hydrophobic groups. At values of $\chi_R > \chi_R^{sat}$, lateral steric interactions among adsorbed proteins may also contribute to decreasing the amount of desorption.[53,54]

**Analysis of Adsorption with the Hard-Sphere Model.** We wished to analyze whether, and to what extent, proteins that are adsorbed to hydrophobic surfaces undergo conformational rearrangements. We estimated the extent of these rearrangements based on the deviation of our data from the predictions of a simple hard-sphere model. Below, we begin by describing the assumptions of the hard-sphere model and the different ways in which hard spheres can pack at a surface. We use the information on the packing of hard spheres to calculate the number of lattice sites of the SAM that are occupied by the hard spheres. After the introduction of the theoretical predictions of the model, we convert the experimentally mea-

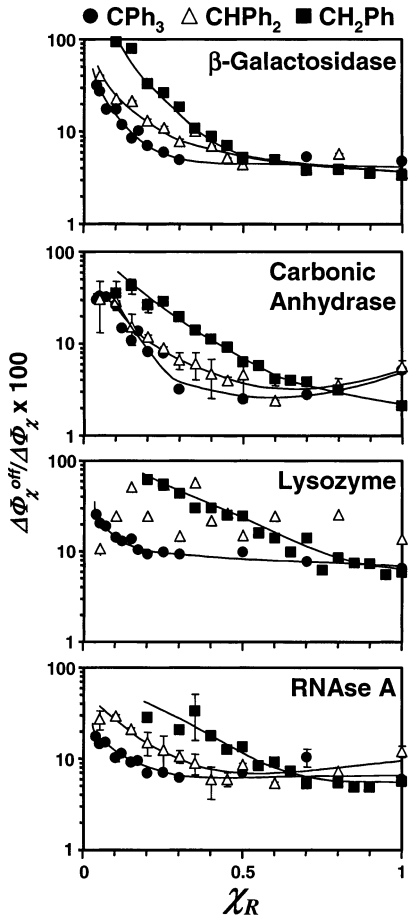


**Figure 9.** Plots of $\Delta\Phi_\chi^{off}/\Delta\Phi_\chi \times 100$ (the percentage of adsorbed protein that desorbed) as a function of $\chi_R$ with R = $CPh_3$ (●), $CHPh_2$ (△), and $CH_2Ph$ (■) for the four indicated proteins. The values of $\Delta\Phi_\chi^{off}$ and $\Delta\Phi_\chi$ were measured from each sensorgram as indicated in Figure 4. The values of $\Delta\Phi_\chi^{off}/\Delta\Phi_\chi \times 100$ obtained with the lowest values of $\chi_R$ were not plotted. We plot the values of $\Delta\Phi_\chi^{off}/\Delta\Phi_\chi \times 100$ on a log scale to facilitate the visualization of the data points. The error bars represent the measured extremes; in most cases, the range is smaller than the height of each point. The uncertainty in the values of $\chi_R$ is undefined. The lines connecting the data are drawn only to guide the eye.

sured quantities to average numbers of occupied lattice sites on the gold surface (defined as the site where the sulfur atom of the alkanethiol coordinates the gold) to allow us to quantify the variation of the experimental data from the calculated ones. We then describe the dependence of the amount of adsorbed protein on the concentration of protein in solution. We conclude this discussion with estimates of the average number of hydrophobic groups that interact with each molecule of adsorbed protein.

In the hard-sphere model, proteins are approximated as hard spheres that (i) adsorb to the surfaces randomly and irreversibly and (ii) cannot change their position once they come in contact with the surface (random sequential adsorption, Figure 2).[40,44] In this model, at most 54% of the surface is covered with adsorbed protein (as a hard sphere) because of excluded area effects.[40,41]

Theoretically, the most dense arrangement of hard spheres on a surface is HCP; in this configuration, the projected area of the spheres covers 91% of the available area.[41,54] Although the HCP limit is never reached experimentally in our studies, it provides a useful point of comparison for cases in which proteins adsorb at densities higher than those predicted by the RSA model. In the following discussion, we show that the predictions

(52) The scatter in the plot of $\Delta\Phi\chi_{off}/\Delta t$ vs $\chi_R$ for lysozyme with SAMs terminated with $ChPh_2$ groups is an artifact that we cannot account for.

(53) Tilton, R. D. *Mobility of Biomolecules at Interfaces*; Malmsten, M., Ed.; Marcel Dekker: New York, 1998; Vol. 75, pp 363−407.

(54) Tilton, R. D.; Gast, A. P.; Robertson, C. R. *Biophys. J.* **1990**, *58*, 1321−1326.

**Table 1. Parameters Determined Using the Hard-Sphere Model**

| protein | source | MW (kDa) | pI | sphere volume ($nm^3$)[d] | sphere radius (nm)[e] | lattice sites HCP[f] | radius RSA (nm)[g] | lattice sites RSA[g] |
|---|---|---|---|---|---|---|---|---|
| $\beta$-galactosidase (as tetramer)[a] | *Escherichia coli* | 540 | 4.1 | 620 | 5.3 | 485 | 7.2 | 817 |
| carbonic anhydrase[b] | cow | 30 | 5.9 | 34 | 2.0 | 69 | 2.7 | 117 |
| lysozyme[c] | hen | 14 | 11.1 | 16 | 1.6 | 42 | 2.1 | 70 |
| RNAse A[c] | cow | 14 | 9.5 | 16 | 1.6 | 42 | 2.1 | 70 |

[a] Jacobson, R. H.; Zhang, R. F.; DuBose, R. F.; Matthews, B. W. *Nature* **1994**, *369*, 761−766. [b] Erikson, A. E.; Jones, T. A.; Liljas, A. *Proteins*: *Struct., Funct., Genet.* **1988**, *4*, 274−283. [c] Shirahama, H.; Lyklema, J.; Norde, W. *J. Colloid Interface Sci.* **1990**, *139*, 177−187. [d] The approximate volume of each molecule of protein was calculated using the density of 1.34 g/$cm^3$ for each protein. [e] The radius of the hard sphere that was determined from the calculated values of the molecular volume. [f] The number of lattice sites per protein was calculated from the area of the circle projected by each hard sphere; the values were divided by 0.91 to correct for the packing in a HCP monolayer. [g] In the hard-sphere model, proteins adsorb to the surface by RSA in which at most 54% of the surface can be covered by proteins. The number of lattice sites per hard sphere was divided by 0.54. Hence, the values of the radii were corrected to account for this difference.

of the RSA model can be exceeded, and those of the HCP monolayer approached, when proteins adsorb from solutions at high concentrations.

We calculated the average number of lattice sites of the SAM per adsorbed hard-sphere protein and then corrected the values for the limits of the HCP monolayer ($L_{HCP}$) and the RSA approximation ($L_{RSA}$) (Figure 2). The calculation of $L$ was performed in the following manner: (i) the volume of each protein (described as a hard sphere) was calculated from the known values of the density and molecular weight of each protein (Table 1); (ii) the calculated volumes of the hard spheres were used to determine the radii ($r$) of the spheres; (iii) the radii were used to calculate the areas of the projections of the hard spheres on the surface; (iv) the areas of the projections of the hard spheres were divided by 0.2 $nm^2$ (the area of one lattice site of the terminal group in the SAM) to obtain the number of lattice sites of the SAM per hard sphere; (v) $L_{HCP}$ was calculated by dividing the number of lattice sites per hard sphere by 0.91; (vi) the values of $L_{RSA}$ were obtained by dividing the number of lattice sites per hard sphere by 0.54 (Table 1).[55]

The experimental values of the number of lattice sites per protein ($L'$) were determined in several steps. We converted the values of $\Delta\theta$ to those of the coverage of the surface by the protein ($\Gamma$) using a relationship proposed previously (eq 2).[18,56]

$$\Gamma\ (\text{ng/cm}^2) = 900\ (\text{ng/deg cm}^2)\ \Delta\Phi\ (\text{deg}) \qquad (2)$$

The number of protein molecules per $cm^2$ was obtained by multiplying eq 2 by Avogadro's number, dividing by the molecular weight of the protein (MW (g/mol) in eq 3), and correcting for the use of grams and nanograms.

$$\text{proteins/cm}^2 = \Delta\Phi\ (5.42 \times 10^{17}\ \text{proteins mol/g cm}^2\ \text{deg})/\text{MW} \qquad (3)$$

The number of alkanethiolates per $cm^2$ was estimated at $5 \times 10^{14}$ from the lattice constant of the gold and electron diffraction measurements of SAMs; the surface area of one terminal group is 0.2 $nm^2$.[57] We thus estimated the number of lattice sites per protein ($L'$) by dividing the number of alkanethiolates per $cm^2$ by the number of protein molecules per $cm^2$ (eq 4).

$$L' = \text{lattice sites/protein} = (9.3 \times 10^{-4}\ \text{lattice sites deg mol/protein g})(\text{MW})/\Delta\Phi \qquad (4)$$

The measured values of $L'$ were larger than the ones predicted with the RSA hard-sphere model ($L_{RSA}$) by at least a factor of 1.7−3.0 for each protein when $\chi_R \geq \chi_R^{sat}$ (Table 2). We suggest that the differences between the values of $L'$ and $L_{RSA}$ reflect conformational rearrangements and spreading of adsorbed proteins on the surfaces of SAMs.

**Table 2. Approximate Values of $L'/L_{RSA}$, $r'/r_{RSA}$, and $r'$ (Figure 2A)[a]**

| protein | $L'/L_{RSA}$[b] | $r'/r_{RSA}$[c] | $r'$ (nm)[d] |
|---|---|---|---|
| $\beta$-galactosidase | 2.9 | 1.7 | 8.8 |
| carbonic anhydrase | 2.0 | 1.4 | 2.7 |
| lysozyme | 1.7 | 1.3 | 2.0 |
| RNAse A | 2.6 | 1.6 | 2.5 |

[a] All values in this table were determined for surfaces with $\chi_{CPh_3} = 1$. At $\chi_R = 1$, the values of $\Delta\Phi_\chi$ converged for all R groups; hence, it is suitable to use the values obtained with $CPh_3$ groups to infer trends obtained with the other two groups. [b] Calculated using eq 4 and the values in Table 1. [c] Calculated using eq 5. [d] Values of $r'$ were obtained by multiplying $r'/r_{RSA}$ by the calculated values of $r_{RSA}$ listed in Table 1.

We assume that the projection of the adsorbed protein is circular and use the values of $L'$ to determine the radius ($r'$) of that circular projection. The ratio of $r'$ to the radius of the hard sphere (determined from the RSA model ($r_{RSA}$), Figure 2) can be determined from values of $L'$ and $L_{RSA}$ (eq 5).

$$\frac{r'}{r_{RSA}} = \sqrt{\frac{L'}{L_{RSA}}} \qquad (5)$$

For each protein, the values of $L'/L_{RSA}$ and $r'/r_{RSA}$ are similar for each hydrophobic group for $\chi_R = 1$ because the surfaces are saturated with hydrophobic groups and adsorb similar amounts of proteins (Table 2).

*Coverage Depends on the Concentration of Protein in Solution*. Our results indicate that adsorbed proteins take on conformations that are different and occupy larger areas than those predicted by the hard-sphere model (Table 2) by factors of 2−3. Values of $\Delta\Phi$ are correspondingly lower than those predicted by assuming that the proteins adsorb as hard spheres (see Supporting Information).[58] The values of $\Delta\Phi$ and $L$ predicted for carbonic anhydrase by the hard-sphere model were reached only during experiments with the highest concentrations of protein (Figure 10). The

(55) The analysis that we carried out and the experimental data that we have gathered do not allow us to distinguish between films of adsorbed protein that are continuous or films in which individual protein molecules adsorb in discrete islands. The deviation of the measured values of $\Delta\Phi$ from the predicted ones (Figure 10), however, is strong indication that the proteins do change shape on the surface.

(56) Sigal, G. B.; Mrksich, M.; Whitesides, G. M. *Langmuir* **1997**, *13*, 2749−2755.

(57) Strong, L.; Whitesides, G. M. *Langmuir* **1988**, *4*, 546−558.

(58) The values of $\Delta\Phi$ were calculated using eq 3. The values of $L_{RSA}$ from Table 1 were converted to values of proteins/$cm^2$. With eq 3, the predicted values of proteins/$cm^2$ can be used to determined the values of $\Delta\Phi$ predicted by the RSA model.

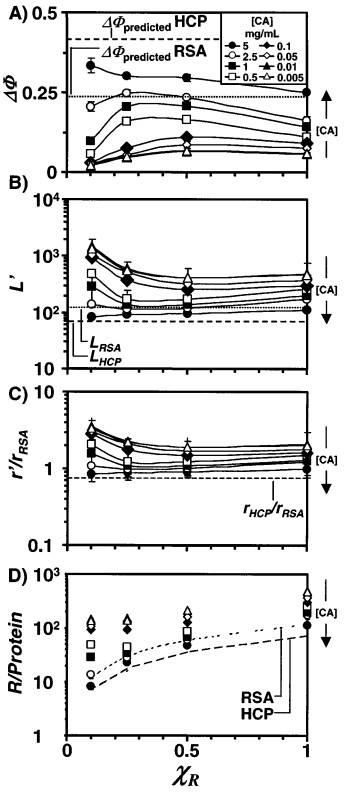


**Figure 10.** Plots of $\Delta\Phi$ (A), $L'$ (B), $r'/r_{RSA}$ (C), and R/Protein (D) for the adsorption of CA to mixed SAMs of $HS(CH_2)_{11}(EG)_6OCHPh_2$ and $HS(CH_2)_{11}(EG)_3OH$ as a function of $\chi_{CHPh_2}$. In plots A, B, and D, dashed lines indicate the values of $\Delta\Phi$, $L$, and R/Protein predicted for layers that were close packed (HCP) or that adsorbed according to the RSA model. We plot the data on a logarithmic scale to aid in their visualization; the lines connecting the points are drawn only to guide the eye. The error bars represent the measured extremes; in most cases, the range is smaller than the height of each point. The uncertainty in the values of $\chi_R$ is undefined. The legend in (A) is the same for all panels. In (A), the solutions of protein (at the indicated concentrations, mg/mL) were allowed to flow over the surface of the SAMs for 20 min at a flow rate of 10 $\mu$L/min (all other SPR measurements reported in this paper were conducted at 5 $\mu$L/min). The layers of adsorbed protein were rinsed with buffer for 12 min; the rest of the protocol is the same as that used to collect the data plotted in Figures 4 and 5. (B) The values of $\Delta\theta$ plotted in (A) were converted to values of $L'$ using eq 4. The legend is the same as that in (A). In (C), the values of $L'$ were used in conjunction with the values of $L_{RSA}$ to determine $r'/r_{RSA}$ (eq 5) at each value of $\chi_{CHPh_2}$. The dashed line corresponds to the value of $r_{HCP}/r_{RSA}$ for a HCP layer of protein. (D) The values of $L'$ in (B) were converted to R/Protein with eq 6 (see text). The lines connecting the data are drawn only to guide the eye. The arrows on the right abscissa indicate the trend in increasing concentration of protein in each panel.

dependence of $\Delta\Phi$ on the concentration of protein in solution is typical of processes that do not follow the Langmuir model.

*Approaching the Limits of the Hard-Sphere Model.* We examined the influence of the concentration of protein in solution on the amount of protein adsorbed using carbonic anhydrase; this medium-sized globular protein serves as a useful model for studying the adsorption of proteins with conformations that are compatible with the hard-sphere model. The use of solutions of carbonic anhydrase at high concentrations (>1 mg/mL, >0.03 mM) resulted in values of $\Delta\Phi_\chi$ that approached the predictions of a HCP monolayer (Figure 10). The adsorption of lysozyme, pancreatic ribonuclease, and plasma proteins to surfaces at densities near the HCP limit have been reported before.[59−63] Under the conditions of these experiments, we hypothesize that the dissolved proteins reach the surface by diffusion, adsorb, and move laterally into a close-packed array at a rate that is overall faster than the rate at which adsorbed molecules undergo conformational changes and spread on the surface (Figures 2 and 10A,B).[46,53]

Interestingly, when using solutions of carbonic anhydrase at high concentrations, we measured the largest values of $\Delta\Phi_\chi$ on surfaces with $\chi_{CHPh_2} = 0.1$ rather than $\chi_{CHPh_2} = 1$. On surfaces with $\chi_{CHPh_2} = 0.1$, the proteins adsorbed with projected areas that compared well with those predicted by the hard-sphere model (RSA and HCP) (Figure 10).

*The Number of R Groups Contacted by a Protein.* Using the values of $L_{RSA}$, we estimated the number of R groups covered by the projection of each protein in the adsorbed layer (R/Protein). We define the values of R/Protein according to eq 6 by multiplying $L'$ by $\chi_R$.

$$\text{R/Protein} = (9.3 \times 10^{-4})(\chi_R)(\text{MW})/\Delta\Phi \qquad (6)$$

The high values of R/Protein obtained with $\chi_R \leq 0.05$ are probably an artifact of the division by the small values of $\Delta\Phi$ measured in those cases (Figure 11). The increase in R/Protein with increasing $\chi_R$ is expected because more R groups are present at the surface. We compare the experimental values of R/Protein to those predicted with the hard-sphere model by multiplying $L_{RSA}$ (Table 1) by $\chi_R$.

As expected, the minima in R/Protein increased with the molecular weight of the proteins and decreased with the size of the hydrophobic group (Table 3). In Figure 11, the minima of R/Protein were higher than the predictions of the hard-sphere model, suggesting that even on those surfaces, the proteins spread on adsorption. Using concentrated solutions of carbonic anhydrase led to values of R/Protein that were 30% larger than those predicted for a HCP monolayer of protein (Table 2). We infer that a maximum of eight $CHPh_2$ groups are required to adsorb one molecule of carbonic anhydrase (from a 5 mg/mL solution) on a SAM with $\chi_{CHPh_2} = 0.1$; we predict that in a HCP monolayer, six $CHPh_2$ groups are required to adsorb one molecule of carbonic anhydrase on such a surface.

## Conclusions

The major advantage of the mixed SAMs that we have described is that they make it possible to place hydrophobic groups with a well-defined structure at a surface with a well-defined average surface density. We have shown that the amounts of adsorbed protein can be controlled by the density of the hydrophobic groups at the surfaces. In the current system, it was not possible to observe the adsorption of one protein molecule to one hydrophobic group; the minimum number of groups inferred (six $CHPh_2$ groups at $\chi_{CHPh_2} = 0.1$ for adsorption of carbonic anhydrase) is still uninterpretable in terms of detailed molecular interactions. Achieving the goal of developing a system in which one protein molecule will adsorb reversibly, by hydrophobic interactions, to one hydrophobic group on an otherwise nonadsorbing surface will probably require tethering a hydrophobic molecule with the equivalent

(59) Norde, W. *Adv. Colloid Interface Sci.* **1986**, *66*, 267−340.
(60) Norde, W.; Lyklema, J. *J. Colloid Interface Sci.* **1978**, *66*, 257−265.
(61) Robeson, J. L.; Tilton, R. D. *Biophys. J.* **1995**, *68*, 2145−2155.
(62) Robeson, J. L.; Tilton, R. D. *Langmuir* **1996**, *12*, 6104−6113.
(63) Brash, J. L.; Lyman, D. J. *J. Biomed. Mater. Res.* **1969**, *3*, 175−189.

**Table 3. Minimum Values of R/Protein for the Adsorption of Each Protein on Each Type of Mixed SAM[a]**

| | R=$CPh_3$ | | R=$CHPh_2$ | | R=$CH_2Ph$ | |
|---|---|---|---|---|---|---|
| protein | R/Protein | $\chi_{CPh_3}$ | R/Protein | $\chi_{CHPh_2}$ | R/Protein | $\chi_{CH_2Ph}$ |
| $\beta$-galactosidase (as tetramer) | 305 | 0.05 | 461 | 0.10 | 966 | 0.35 |
| carbonic anhydrase | 51 | 0.15 | 50 | 0.20 | 79 | 0.45 |
| lysozyme | 25 | 0.05 | 65 | 0.10 | 101 | 0.90 |
| RNAse A | 26 | 0.05 | 70 | 0.20 | 140 | 0.70 |

[a] The minima were determined from the plots of R/Protein vs $\chi_R$ in Figure 11. The values of $\chi_R$ at which these minima occurred are also indicated.

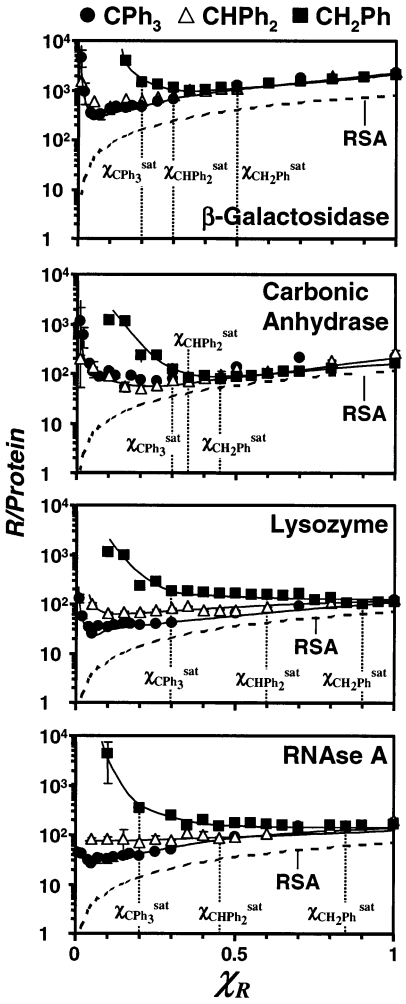


**Figure 11.** Plots of R/Protein vs $\chi_R$. The values of $\Delta\Phi_\chi$ measured on each mixed SAM were converted to R/Protein using eq 6. The dashed line was obtained by multiplying the predicted values of $L_{RSA}$ by $\chi_R$. The lines connecting the data are drawn only to guide the eye. We label the values of $\chi_R^{sat}$ from Figures 6 and 7.

hydrophobic area of 5−6 benzyl groups to the surface. The constraints on shape, flexibility, and molecular structure in this type of system remain to be defined.

The hard-sphere model provides a useful benchmark for the interpretation of data on the hydrophobic adsorption of protein. The area of the surface occupied by an adsorbed protein ranged from ~3−5 times that expected for a HCP monolayer and ~2−3 times that expected from the RSA model (Figure 2).

We interpret the deviation of our data from the predictions of the hard-sphere model to mean that in most circumstances, adsorption of protein proceeds by an initial adsorption step that is followed by its spreading and denaturation in processes that are more rapid than lateral diffusion and formation of ordered surface phases. The use of solutions of carbonic anhydrase at high concentration allowed the density of the adsorbed proteins to approach that expected for a HCP phase. Surfaces with low densities of hydrophobic groups are also useful to minimize the extent of conformational rearrangement in the adsorbed proteins.

Mixed SAMs with low values of $\chi_R$ and large hydrophobic groups offer the most interesting opportunities for further research, because they might make it possible to study the interaction of proteins with a single, isolated, hydrophobic group. In that system, it would be essential to minimize the possibility of phase separation. Generating a true statistical distribution of groups on the surface of a SAM would probably be best accomplished by starting with mixed SAMs of $HS(CH_2)_{11}O(EG)_3OH$ and $HS(CH_2)_{11}O(EG)_6OCH_2COOH$ (where the SAM is probably ideally mixed) and attaching the hydrophobic group in a later step.[64]

This experimental system does not define the structure of the "products" of adsorption, that is, the conformations and structures of adsorbed and possibly denatured or rearranged proteins, and it does not define the positions of the hydrophobic groups relative to one another in the plane of the surface. The system does, however, bring many other aspects of the experiment under control and provides the best-defined system now available for studying protein adsorption to hydrophobic surfaces.

Probably the most serious ambiguity in this system as it is currently constructed has to do with the potential for heterogeneity in the SAM due either to statistical clustering of R groups or to microphase separation in the two-component mixed SAMs. These effects could be minimized by studying systems with low values of $\chi_R$ ($\chi_R \leq 0.1$). The studies described here examined the full range of $\chi_R$ from 0.0 to 0.1, but an important conclusion for future work is the desirability of focusing on the lower end of the range.

## Materials and Methods

**Materials.** Lysozyme (L6876; EC 3.2.1.17), ribonuclease A (R5125; EC 3.1.27.5), bovine carbonic anhydrase (C3934; EC 4.2.1.1), $\beta$-galactosidase (G6008; EC 3.2.1.23), and phosphate-buffered saline packets (P3813) were purchased from Sigma and used as received. Proteins were dissolved in filtered PBS and filtered through 0.22 $\mu$m units before use.

**Preparation of SAMs.** Planar substrates were prepared by evaporation of titanium (15 Å) and gold onto glass slides (380 Å for SPR experiments) or silicon wafers (2000 Å for ellipsometry and contact angle measurements). The metallized substrates were immersed in ethanolic solutions containing mixtures of $HS(CH_2)_{11}EG_6OR$ and $HS(CH_2)_{11}EG_nOH$ (2 mM total thiol) in ethanol for 8 h.

**Contact Angle Measurements.** The receding and advancing contact angles of water on the mixed SAMs (Figure 1) were measured with a Ramé-Hart model 100 contact angle goniometer. Liquid drops were delivered and removed from the surface using a Matrix Technologies Microelectrapipette. The reported values of the contact angles are the averages of three different measurements taken at three different locations on the surface.

(64) Lahiri, J.; Isaacs, L.; Tien, J.; Whitesides, G. M. *Anal. Chem.* **1999**, *71*, 777−790.

**Ellipsometry.** Ellipsometric measurements of the thickness of mixed SAMs presenting trityl groups were performed with a Rudolph Technologies Inc. Research Type 43603-200E thin-film ellipsometer with a wavelength of 6328 Å and an incident angle of 70°. Measurements on the other types of SAMs were made with a Rudolph Technologies Inc. Auto EL thin-film ellipsometer operating at 6328 Å with an incident angle of 70°. The thicknesses of the films were calculated with a three-layer isotropic model (ambient air, SAM, substrate) by assuming refractive indices of 1.00 and 1.45 for the ambient air and the SAM.

**Surface Plasmon Resonance Spectroscopy.** We used the Biacore 1000 instrument (Pharmacia) for all studies. We modified the manufacturer's cartridges to accept our substrates, as described previously.[32,34] The adsorption of protein was measured in situ with SPR using the following protocol: a solution of PBS (pH = 7.4, ionic strength ≈ 154 mM) flowed (5 $\mu$L/min) through a cell (2.4 × 0.5 × 0.05 mm) for 2 min followed by 2 min of buffer containing SDS (10 mg/mL) and an additional 1 min of buffer. The flow cell was then washed with buffer at 150 $\mu$L/min for 3 min. A new cycle was started in which buffer flowed for 2 min before an injection of buffer containing protein (1 mg/mL) for 3 min; buffer was then injected for 4 min to wash the surface. We measured $\Delta\theta$ as the difference between the SPR signal obtained at the end of the last buffer injection and the signal before the injection of protein. In the SPR experiments reported in Figure 10, we used the same protocol with a minor change. The surfaces were washed with buffer containing SDS for 15 min instead of 2 min to ensure the removal of the monolayer of protein. For clarity, we show only the protein injection cycle. Sigal et al. have shown that SDS does not interact with SAMs presenting oligo(ethylene glycol) groups and that the *reversible* interaction of SDS with SAMs increases with the contact angle of the SAMs.[18]

**Acknowledgment.** This work was funded by the National Institutes of Health (GM 30367). We also used shared MRSEC facilities supported by the National Science Foundation and the National Institutes of Health under Awards Number DMR-9400396 and 1 S10 RR01748-01A1, respectively. E.O. acknowledges a predoctoral fellowship from Glaxo Wellcome Inc. C.S.R. and M.M. are grateful to the National Science Foundation and the American Cancer Society, respectively, for postdoctoral fellowships.

**Supporting Information Available:** Detailed description of the synthesis of the alkanethiols. Plots of the measured and predicted values of coverage as a function of molecular volume. This material is available free of charge via the Internet at http://pubs.acs.org.

LA020649C